LABORATORI NAZIONALI DI FRASCATI
SIS – Pubblicazioni

LNF-94/075 (P)
6 Dicembre 1994

Elastic and Inelastic Diffraction of High Energy Hadrons

Andrzej Małecki*

KEN Pedagogical University**, Cracow, Poland
and INFN – Laboratori Nazionali di Frascati, P.O. Box 13, I–Frascati (Roma) Italy

Abstract

An approach to inelastic diffraction based on the concept of equivalence of diffractive states is developed. In the classical description of Good and Walker, the inelastic diffraction originates from the diversity of elastic scatterings in the initial and final state Δt. We cosider a multi-channel correction, accounting for intermediate transitions inside the equivalence class. This correction can be factorized yielding the diffraction amplitude in the form $N\Delta t$, to be taken in the 'diffractive limit': $N \to \infty, \Delta t \to 0$ such that $N\Delta t$ is finite. We analyse elastic scattering and the inclusive inelastic diffraction cross-sections for $p-p$ and $p-\bar{p}$ collisions, in the range of c.m. energy $\sqrt{s}$= 20 - 1800 GeV . We claim that the angular distribution of the inclusive inelastic diffraction at small momentum transfers is determined by elastic scattering in the transition region between the forward peak and the minimum. This is successfully verified in experiment. The detailed comparison with the Good-Walker description, with emphasis on advantages of our approach, is presented.

PACS.: 13.85.-t; 03.80.+r, 11.80.-m

(Submitted to Physical Review D)

⋆ On leave of absence from H. Niewodniczański Institute of Nuclear Physics, Kraków.
⋆⋆ Address: Institute of Physics and Computer Science, ul. Podchorążych 2,
30-084 Kraków, Poland.
E-mail: AMALECKI@VSB01.IFJ.EDU.PL and MALECKI@LNF.INFN.IT

1 Introduction

In describing nuclear and hadronic collisions one often encounters the term 'diffraction'-which originates from classical optics. Its use is motivated by striking analogies between light scattering in optics and particle scattering in wave mechanics. Historically [1], diffraction was synonymous to scattering in general. Nowadays [2], 'diffraction scattering' customarily refers to a limited class of phenomena which occur in medium-energy nuclear and high-energy hadron collisions. The sufficient energy of collision allows there an opening of a variety of inelastic channels which in turn implies strong absorption since the presence of competing reactions results in a considerable depletion of the particle flux in the elastic channel. Such conditions are analogous to those for diffraction of light by opaque or partially transparent objects in optics.

The diffraction of light on an obstacle leads to a structured penumbra (instead of the darkness expected in geometrical optics) resulting from the alternating constructive and destructive interference of deflected waves. The diffractive analogy in nuclear and hadron physics consists in a substantial presence of elastic scattering (and other two-body channels) where very little would naively be expected in violent collisions. It also refers to the behaviour of the differential cross-section which is strongly peaked in the forward direction and often appears as a series of maxima and minima. Another 'diffractive' phenomenon is a slow variation with energy of the integrated cross-sections which means that the geometry of absorption dominates details of intrinsic dynamics.

In the Fraunhofer theory of light diffraction the limitation of a wave front by the diffracting object leads to the scattering amplitude in the form of the two-dimensional Fourier transform of a function describing the geometry of scattering. In quantum-mechanical scattering the geometrical limitation may be transposed into a reduction or truncation of a band of orbital angular momenta consisting of a huge number of partial waves which participate coherently in the interaction. In either case one can establish a simple relation between the geometrical properties of the scatterer and those of the diffraction pattern. The great success of the Glauber model [3] in nuclear scattering and of the Chou-Yang model [4] in hadron collisions represents an astonishing evidence that using optical concepts, reflecting merely the fact that nuclei and hadrons have finite sizes, one can achieve a succesful description of the basic features of their scattering.

Obviously, still many problems, related to the more detailed structure of hadrons, remain. E.g. the hadronic analogy of 'diffractive structure' of the differential cross-section is often obscured since multiple dips and reinforcements may not be present. In fact, numerous dips arising in geometrical models of hadron scattering may be washed out when including the unitarity contributions from multi-particle intermediate states [5]. Thus the optical resemblances of high-energy hadron diffraction should not be overemphasized. There is certainly much more dynamics in this process that could be explained simply in terms of geometrical shapes of absorbing obstacles. The

geometrical picture of diffraction on a grey disc may still be useful for modelling the dominant long-range part of scattering. However, it would be highly desirable to disentangle from the vagueness of geometrical diffraction also phenomena of shorter range related to intrinsic dynamics of colliding particles.

The way in this direction goes through a better understanding of the process of 'diffractive excitation' or 'diffraction dissociation' [6, 7] which involves quasi-elastic transitions with no exchange of quantum numbers. The qualifier 'diffractive' refers here merely to the condition of coherence which must (like in elastic diffraction) be satisfied to assure that the interacting particles do not change their character. In elastic scattering where the intrinsic dynamics is hidden inside geometrical shapes, the analogy between optical and particle diffraction seemed to be complete. On the contrary, the 'inelastic diffraction' has no classical analogy; it appears as a peculiar quantum phenomenon connected with the existence of internal degrees of freedom. Phenomenologically [8], the inelastic diffractive channels are characterized by a slow variation with energy of their cross-sections, i.e. by the energy dependence typical of elastic scattering. Indeed, the states produced in these channels have dominant quantum numbers corresponding to the ground state. All other channels where cross-sections drop rapidly with increasing energy are referred to as non-diffractive.

The requirement of quasi-elasticity or 'diffractiveness' of an inelastic transition can be incorporated into a theoretical formalism in either of two ways. In the t-channel approach, inelastic diffraction is described in terms of the exchange of Pomeron, an hypothetical object carrying vacuum quantum numbers. Most papers, inspired by great successes of Regge theory, follow this method [9]. Another approach which is used in this paper, is that of the s-channel. It is based on the presumed relation of equivalence [5] between the initial (ground) state and the states involved in diffractive channels. This means that the Hilbert space of physical states is decomposable into subspaces of diffractive and non-diffractive states. This assumption is taken so much for granted that it is often not stated explicitly.

In order to reveal the equivalence of states one must depart from the representation of physical states as eigenstates of the hadronic Hamiltonian, in which each state is an equivalence class for itself. One is thus looking for a suitable unitary transformation which allows to expand the physical states in terms of the transposed states. The best known transformation, aimed for the description of diffraction, is that of Good and Walker [10] who imposed on the new base states to be eigenstates of the scattering operator. Their approach,referred to as the method of 'diffractive eigenstates', is remainded in Section 2. It should be pointed out that this approach constitutes the ground for the geometrical models of diffraction (e. g. those of Chou-Yang and Glauber), diffractive eigenstates being there identified as the states describing configurations of hadronic (or nuclear) constituents with definite impact parameters.

The natural base for describing 'inelastic diffraction' is obtained through a unitary transformation of physical states such that the transforming operator is reducible in the Hilbert space. As discussed in Section 3, we do not additionally require that the

base states diagonalize the scattering operator. An obvious advantage of rejecting this restriction consists in accounting for intermediate virtual transitions inside the set of diffractive states. Apparently the resulting expressions are quite complicated. However, we were able to show that if the diffractive subspace contains a huge number of states N, the effect of non-diagonal transitions can be factorized: the diffractive transition amplitude has the form $N\Delta t$ where Δt represents a diversity of diagonal matrix elements of the scattering operator over the set of equivalent diffractive states. Such expressions are to be considered in the 'diffractive limit'[5]: $N \to \infty, \Delta t \to 0$ under requirement that $N\Delta t$ is finite. Diffraction thus arises as infinite sum of the infinitesimal contributions from all intermediate states belonging to the diffractive equivalence class.

The general formulae derived in Section 3 are further elaborated in Section 4. We consider there a simple model of diffractive states. They are imagined as built of a hadron bulk (representing the ground state) and of some quanta ('diffractons') corresponding to diffractive excitations. The collisions of hadrons is treated in an analogue model as the scattering of a plane wave off a scatterer composed of two excited hadronic cores. The two-hadron bulk and the density distribution of diffractons inside the core are assumed to have Gaussian shapes. Their radii $R_0 > R_1$ are to be determined from fitting to experimental data. This semiphenomenological model thus explicitly includes the two sources of diffraction: the geometrical diffraction on an absorbing hadronic bulk and the dynamical diffraction corresponding to intermediate transitions (modelled with the aid of diffractons) between equvalent states.

The aim of our calculations was two-fold: to confront theory with experiment and to compare various theoretical approaches between each other. We analyse elastic scattering and the inclusive inelastic diffraction cross-sections for $p - p$ and $p - \bar{p}$ collisions, in the range of c.m. energy $\sqrt{s}$= 20 - 1800 GeV , covered by the measurements carried out at the ISR, SPS and Tevatron colliders [11] - [16]. In all cases, the application of our two-component model is very successful. In elastic scattering, the single minimum observed experimentally is explained as a multichannel interference effect due to scattering off 'diffractons' in the presence of the hadronic bulk. The same effect determines the angular distribution of inclusive inelastic diffraction at low momentum transfers. The detailed discussion of these results ,with emphasis on advantage of our description of diffraction with respect to the traditional Good-Walker approach, is presented in Section 5.

2 Method of diffractive eigenstates

Consider a unitary transformation of the physical states

$$| j\rangle \rightarrow | Uj\rangle \tag{1}$$

and of the scattering operator

$$T \rightarrow T_0 = U^\dagger T U. \tag{2}$$

Any state can be expanded in terms of the new base states, e.g. for the initial state one has:

$$| i\rangle = \sum_{|j\rangle} U^\star_{ij} \ | Uj\rangle \tag{3}$$

where

$$U_{ij} \equiv \langle i \mid U \mid j\rangle \tag{4}$$

is the matrix element of the unitary transformation operator.

The transition amplitude can be written in terms of the matrix elements of the scattering operator in the new base:

$$T_{fi} \equiv \langle f \mid T \mid i\rangle = \sum_{|j\rangle,|k\rangle} U_{fk}\, U^\star_{ij}\, t_{kj} \tag{5}$$

where

$$t_{kj} \equiv \langle Uk \mid T \mid Uj\rangle = \langle k \mid T_0 \mid j\rangle \tag{6}$$

Notice that the summations in the above equations extend over all physical states.

2.1 Transformation of Good and Walker

The general transition amplitude (5) can be simplified by considering the unitary transformation which diagonalizes the scattering operator:

$$T \mid Uj\rangle = t_j \ | Uj\rangle \tag{7}$$

which is equivalent to

$$T_0 \mid j\rangle = t_j \mid j\rangle \tag{8}$$

i.e. the transformed scattering operator is diagonal in physical states. Such a unitary transformation $U = U_{GW}$, first considered by Good and Walker [10], exists since the scattering operator is normal. Indeed the unitarity of the collision operator $S = 1 + iT$ implies:

$$TT^\dagger = T^\dagger T = i(T^\dagger - T)$$

and

$$T_0 T_0^\dagger = T_0^\dagger T_0 = i(T_0^\dagger - T_0). \tag{9}$$

The base states $\mid U_{GW}j\rangle$ were named 'eigenstates inside nuclear matter'[10]. They are also referred to as 'diffractive states' or better 'diffractive eigenstates'. Using this base Eq. (5) is simplified to the single sum over states:

$$T_{fi} = \sum_{|j\rangle} U_{fj}\, U_{ij}^{\star}\, t_j \tag{10}$$

and, in particular, the elastic scattering amplitude appears in the form of an average of the eigenvalues t_j over the set of physical states:

$$T_{ii} = \sum_{|j\rangle} \mid U_{ij} \mid^2 t_j \tag{11}$$

with the weigth $|U_{ij}|^2$ which satisfies $\sum_{|j\rangle} |U_{ij}|^2 = 1$.

From Eq.(10) one can see that if the eigenvalues t_j were the same for all states then the inelastic amplitude would vanish because of unitarity of U. Thus the inelastic scattering arises from the diversity of the eigenvalues t_j which corresponds to various absorptions of diffractive eigenstates as the components of the initial state. However, this mechanism of inelasticity is very general; it applies to any inelastic scattering and not exclusively to inelastic diffraction.

The diagonalization (8) was replaced by Białas, Czyż and Kotański [18] with a weaker assumption of diagonalization of the scattering operator in a particular class of states only. Denoting the chosen subset of states by [D] and its orthogonal complement by [~D] one has for any state $\mid j\rangle \in [D]$:

$$T_0 \mid j\rangle = t_j \mid j\rangle + \sum_{|k\rangle \in [\sim D]} t_{kj} \mid k\rangle. \tag{12}$$

The states belonging to [D] will be called diffractive states and those from[$\sim D$] are referred to as non-diffractive. Eq. (12) can be interpreted as the requirement that the base states of the diffractive sector are subject only to elastic scattering which arises from absorption related to the production of non-diffractive states.

If the transition takes place between two diffractive states, i.e. when $\mid i\rangle \in [D]$ and $\mid f\rangle \in [D]$, one has then:

$$T_{fi} = \sum_{|j\rangle \in [D]} U_{fj}\, U_{ij}^{\star}\, t_j \tag{13}$$

and

$$T_{ii} = \sum_{|j\rangle \in [D]} |U_{ij}|^2\, t_j \tag{14}$$

which only seemingly is the same as Eqs. (10) and (11) since the summation over states is now restricted to the class [D] of diffractive states.

From Eq. (13) one may easily obtain the inclusive inelastic cross-section of diffractive transitions:

$$\sum_{|f\rangle \neq |i\rangle} |T_{fi}|^2 = \sum_{|j\rangle \in [D]} |U_{ij}|^2 \, |t_j|^2 - |T_{ii}|^2 = \sum_{|j\rangle \in [D]} |U_{ij}|^2 \, |T_{ii} - t_j|^2 \qquad (15)$$

Thus while the elastic scattering amplitude is an average value of the absorption coefficients t_j, the inclusive cross-section of inelastic diffraction appears as their dispersion.

The approach of Good and Walker constitutes the ground for the geometrical models of diffraction. In these models one takes for granted that the interaction of high-energy composite hadrons depends on the distribution of their constituents in the impact parameter plane only. There is an implicit assumption that a very fast projectile passing through hadronic medium is outside of the target long before the changes it induces in the medium take place. Thus when the projectile interacts with any of the target constituents, the others are fixed in their positions and can be considered inactive spectators. This means that it is just the states $\mid \vec{b}_1, \ldots, \vec{b}_n\rangle$, describing the configurations of hadron constituents with definite impact parameters, which are eigenstates of diffraction. Eq. (12) reads then :

$$T \mid \vec{b}_1, \ldots, \vec{b}_n\rangle = t(\vec{b}, \vec{b}_1, \ldots, \vec{b}_n) \mid \vec{b}_1, \ldots, \vec{b}_n\rangle + \sum_{|k\rangle \in [\sim D]} t_{kj} \mid Uk\rangle, \qquad (16)$$

$\vec{b}$ being the impact parameter which describes the trajectory of the projectile hadron.

The transition amplitude can thus be written in a more familiar form:

$$T_{fi}(\vec{b}) = \sum_{n=1}^{\infty} P_n \int d^2b_1, \ldots, d^2b_n \; \Phi_f^* \, t(\vec{b}, \vec{b}_1, \ldots, \vec{b}_n) \; \Phi_i \qquad (17)$$

where Φ_f, Φ_i are the wave functions, e.g. $\Phi_i(\vec{b}_1, \ldots, \vec{b}_n) \equiv \langle \vec{b}_1, \ldots, \vec{b}_n \mid i\rangle$, and P_n is the probability to find the configuration of n constituents. Assuming the celebrated cluster form of the hadronic profile [3, 7]:

$$t(\vec{b}, \vec{b}_1, \ldots, \vec{b}_n) = i[1 - \prod_{k=1}^{n} [1 - \gamma(\vec{b} - \vec{b}_k)]] \qquad (18)$$

one obtains then the nuclear Glauber model [3] with $P_n = \delta_{nA}$ and the Chou-Yang model [4] with the Poissonian P_n.

2.2 Normal part of the unitary transformation

It is convenient to extract from the unitary operator U the identity transformation:

$$U \equiv 1 - \Lambda. \qquad (19)$$

The operator Λ satisfies the relation of normality:

$$\Lambda\Lambda^\dagger = \Lambda^\dagger\Lambda = \Lambda + \Lambda^\dagger. \tag{20}$$

In terms of the matrix elements the two last equations read:

$$U_{kj} = \delta_{kj} - \Lambda_{kj},$$

$$|U_{kj}|^2 = |\Lambda_{kj}|^2 + (1 - 2Re\Lambda_{jj})\delta_{kj} \tag{21}$$

and

$$\Lambda_{kj} + \Lambda^*_{kj} = \sum_{|l\rangle} \Lambda_{kl}\Lambda^*_{jl}. \tag{22}$$

Using the Ansatz (19) the diffractive transition amplitude (13) is

$$T_{fi} = t_i\delta_{fi} - \Lambda_{fi}\, t_i - \Lambda^*_{if}\, t_f + \sum_{|j\rangle\in[D]} \Lambda_{fj}\, t_j \Lambda^*_{ij}$$

or equivalently

$$T_{fi} = t_i\delta_{fi} + \frac{1}{2}(\Lambda_{fi} - \Lambda^*_{if})\,(t_f - t_i) + \sum_{|j\rangle\in[D]} \Lambda_{fj}\,\Lambda^*_{ij}\,[t_j - \frac{1}{2}(t_f + t_i)]. \tag{23}$$

In particular, the elastic scattering amplitude reads

$$T_{ii} = t_i + \sum_{|j\rangle\in[D]} |\Lambda_{ij}|^2 (t_j - t_i). \tag{24}$$

If all Λ_{kj} were small then retaining only the terms linear in Λ (breaking thus unitarity) one would yield the elastic scattering amplitude trivially equal to the eigenvalue of T_0 in the initial state. Instead, the inelastic diffraction amplitude would be proportional to the difference of these eigenvalues in the initial and final state , which is the classical result of Ref.[18]. The last terms of Eqs. (23) and (24) can be considered as the unitarity corrections from the intermediate diffractive states.

For completness we also write down the inclusive cross-section of inelastic diffraction (15) in terms of the operator Λ:

$$\sum_{|f\rangle\neq|i\rangle} |T_{fi}|^2 = \sum_{|j\rangle\in[D]} |\Lambda_{ij}|^2\, |t_j - t_i|^2 - |T_{ii} - t_i|^2. \tag{25}$$

Although the three last equations are equivalent to Eqs.(13),(14) and (15), there can be important differences when the two kinds of expressions are applied to phenomenological analyses. The structure of the Λ-type formulae leaves more room for

suitable choices of the theoretical ingredients. While in the approach using the operator U all the eigenvalues t_j are treated on the same footing, in the Λ-description the ground state eigenvalue t_i is distinguished. One can thus make a particular choice of t_i irrespectively of the form of $t_{j\neq i}$.

The phenomenological form of the density $|U_{ij}|^2$ is constrained only by the normalization to unity. However the density $|\Lambda_{ij}|^2$ is yet not normalized, yielding thus an additional parameter at disposal. In fact, from Eq. (22) one has:

$$\sum_{|j\rangle\in[D]} |\Lambda_{ij}|^2 = 2Re(\Lambda_{ii}) \equiv g_i. \tag{26}$$

From Eq.(21) one gets:

$$(Re\Lambda_{ii} - 1)^2 + Im^2\Lambda_{ii} = |U_{ii}|^2. \tag{27}$$

Because $|U_{ii}| \leq 1$, this implies the constraint:

$$0 \leq g_i \leq 4. \tag{28}$$

Rather a small value of g_i would be expected to reflect the experimental fact that the cross-sections for inelastic diffractive processes are about one order of magnitude smaller than elastic ones. It should also be observed that when $g_i = 1$ the two approaches yield the identical expressions.

3 New approach to diffraction

We will present a new approach to inelastic diffraction which differs essentially from the classical works reminded in Section 2.1 . One emphasized there the properties of the transformed scattering operator T_0 (i.e. its complete or partial diagonalization) rather than the structure of the transforming operator U. A convenient tool in this new direction is Eq.(19) since by splitting the unitary operator in the two parts one arrives to the following decomposition of the scattering operator [5]:

$$T = T_0 - \Lambda T_0 - T_0\Lambda^\dagger + \Lambda T_0 \Lambda^\dagger. \tag{29}$$

We envisage that it is just the three last terms in this expression which describe diffractive processes. All they do contain the operator Λ which is the essential part of the unitary transformation aimed to distinguish between diffractive and non-diffractive channels. We will consider Λ to be a 'soft' operator which induces a 'smooth' transformation of the physical states $|j\rangle$ in the diffractive sector so the transformed states $|Uj\rangle$ are very 'close' to each other. We have seen earlier that the 'strength' of the operator Λ can be controlled with the aid of the parameter g_i. On the other hand, we consider T_0 to be a 'hard' operator which has nothing to do with diffractive processes. It does essentially contribute to a geometrical (long-range) part of elastic scattering which arises as the shadow of a huge number of inelastic (mostly non-diffractive) processes. However, it cannot directly contribute to inelastic diffraction.

In our approach we reject the condition (12) of Section 2 regarding the diagonalization of the scattering operator. First, we consider it as a redundant assumption since the required division of channels into the two classes may be formulated otherwise. Secondly, it screens a part of dynamics. In fact, considering the most general expression:

$$T_0 \mid j\rangle = \sum_{|k\rangle \in [D]} t_{kj} \mid k\rangle + \sum_{|k\rangle \in [\sim D]} t_{kj} \mid k\rangle \tag{30}$$

one reveals there, besides the absorption of non-diffractive origin, also another source of absorption implied by transitions inside the set of diffractive states.

3.1 Equivalence of diffractive states

The fundamental point in the description of diffraction is the presumed existence of two orthogonal subspaces of diffractive and non-diffractive states. This requirement can be rephrased by saying that there exist unitary operators U and $U^\dagger$ which are reducible in the Hilbert space of physical states. This implies the existence of a non-trivial subspace $[D]$ such that for any $|j\rangle \in [D]$ also $|Uj\rangle$ and $|U^\dagger j\rangle$ belong to $[D]$.

In consequence, for any state $|k\rangle$ belonging to the orthogonal complement $[\sim D]$ also $|Uk\rangle$ and $|U^\dagger k\rangle$ will belong to $[\sim D]$. In terms of the matrix elements this reads:

$$\begin{aligned} \langle k \mid Uj\rangle &= \langle j \mid U^\dagger k\rangle^* = 0, \\ \langle k \mid U^\dagger j\rangle &= \langle j \mid Uk\rangle^* = 0 \end{aligned} \tag{31}$$

for any $|j\rangle \in [D]$ and $|k\rangle \in [\sim D]$. A careful inspection of the passage from Eqs. (10) and (11) to Eqs. (13) and (14) indeed reveals that the above relations of orthogonality were implicitly assumed.

Alternatively one may say that the operator U can be decomposed into the direct sum of operators which act on orthogonal subspaces (classes of equivalence) of the physical Hilbert space:

$$U = U_D \oplus U_{\sim D} \equiv U_{DF}. \tag{32}$$

Such an operator will be referred to as the unitary diffractive filter U_{DF}. In the base of physical states the matrix U_{kj} representing U_{DF} has a 'diagonal box' form. Assuming that the initial state belongs to $[D]$ one has then:

$$\begin{aligned} U_{ij} &\neq 0 \quad \rightarrow |\, j\rangle \in [D], \\ U_{ij} &= 0 \quad \rightarrow |\, j\rangle \in [\sim D]. \end{aligned} \tag{33}$$

The complementary subspace $[\sim D]$ of states which are non-diffractive with respect to the set $[D]$ may eventually further be decomposed into smaller classes of equivalence. The matrix U_{kj} would then be made of more than two 'boxes'.

Obviouly the reducibility of U_{DF} implies that the corresponding operators Λ and $\Lambda^\dagger$ will also be reducible in the space of physical states, i.e. the matrix Λ_{kj} is block-diagonal. The property of normality (20) allows their diagonalization. Writing the operator U_{DF} in a manifestly unitary form:

$$U_{DF} = e^{iM},\ M = M^\dagger \tag{34}$$

we have also at disposal the hermitian operator M. There exist the common eigenstates $|\mu\rangle$ for which

$$M \mid \mu\rangle = 2\pi\mu \mid \mu\rangle, \tag{35}$$

$$\Lambda \mid \mu\rangle = (1 - e^{2\pi i\lambda}) \mid \mu\rangle \tag{36}$$

where

$$\mu = \lambda + n;\ n = 0, \pm 1, \pm 2, \ldots;\ 0 \leq \lambda < 1. \tag{37}$$

The states $|\mu\rangle = |\lambda + n\rangle$ are infinitely degenerated with respect to the eigenvalue λ . Thus with each value of λ one can associate a subspace (class of equivalence) and the projector operator

$$P_\lambda = \sum_{n=-\infty}^{\infty} \mid \lambda + n\rangle\langle \lambda + n \mid \tag{38}$$

which projects onto this subspace $[P_\lambda]$.

For each λ one has :

$$[\Lambda, P_\lambda] = [\Lambda^\dagger, P_\lambda] = 0 \tag{39}$$

and

$$\Lambda\, P_\lambda = (1 - e^{2\pi i\lambda})\, P_\lambda,\ \Lambda^\dagger\, P_\lambda = (1 - e^{-2\pi i\lambda})\, P_\lambda. \tag{40}$$

These relations prompt us a possible connection between the eigenspaces $[P_\lambda]$ of the operator Λ and the equivalence of physical states. The states will be said to be equivalent *modulo* Λ if they belong to one of the direct sums:

$$[\lambda] = [P_\lambda] \oplus [P_0] \tag{41}$$

for each $\lambda \neq 0$. Thus for any $|j\rangle \in [\lambda]$ one has

$$|\, j\rangle \;=\; P_\lambda \,|\, j\rangle \;+\; P_0 \,|\, j\rangle \tag{42}$$

or more explicitly

$$|\, j\rangle = \sum_{n=-\infty}^{\infty} \varphi_{\lambda j}(n)\ |\, \lambda + n\rangle \;+\; \sum_{n=-\infty}^{\infty} \varphi_{0j}(n)\ |\, n\rangle \tag{43}$$

where $\varphi_{\lambda j}(n) \equiv \langle \lambda + n \mid j\rangle$. The structure of (43) implies that the set of equivalent (diffractive) states will generally be very numerous which may be related to the compositness of the colliding hadrons.

Since

$$\Lambda \,|\, j\rangle \;=\; (1 - e^{2\pi i\lambda})\, P_\lambda \,|\, j\rangle \tag{44}$$

for any $|j\rangle \in [\lambda]$, the operator Λ is indeed reducible and its matrix elements between non-equivalent states will vanish:

$$\begin{aligned} \Lambda_{kj} \;&=\; (1 - e^{2\pi i\lambda})\, \langle k \mid P_\lambda \mid j\rangle \delta_{\lambda'\lambda} \\ &=\; (1 - e^{2\pi i\lambda}) \sum_{n=-\infty}^{\infty} \varphi^*_{\lambda' k}(n)\, \varphi_{\lambda j}(n)\, \delta_{\lambda'\lambda} \end{aligned} \tag{45}$$

for any $|j\rangle \in [\lambda], |k\rangle \in [\lambda']$.

3.2 Diffractive limit

The states $|U_{DF} j\rangle$ obtained through the unitary transformation wheach reveals the decomposition of the Hilbert space of states into classes of equivalence constitute a natural base for the description of diffraction. The amplitude of diffractive transitions follows then directly from Eq. (5) by restricting the summation over states to the class $[D]$ of diffractive states. Alternatively from Eq. (29) one obtains :

$$T_{fi} \;=\; t_{fi}\delta_{fi} \;-\; \sum_{|k\rangle \in [D]} \Lambda_{fk}\, t_{ki} \;-\; \sum_{|j\rangle \in [D]} t_{fj} \Lambda^*_{ij} \;+\; \sum_{|j\rangle, |k\rangle \in [D]} \Lambda_{fk}\, t_{kj} \Lambda^*_{ij}. \tag{46}$$

The three last terms of (46) can be rewritten as follows:

$$\begin{aligned}
\sum_{|k\rangle\in[D]} \Lambda_{fk}\, t_{ki} &= N_{fi}(T_0)\Lambda_{fi}t_i \\
\sum_{|j\rangle\in[D]} t_{fj}\Lambda^{\star}_{ij} &= \Lambda^{\star}_{if}t_f N^{\star}_{if}(T_0^{\dagger}) \\
\sum_{|j\rangle,|k\rangle\in[D]} \Lambda_{fk}t_{kj}\Lambda^{\star}_{ij} &= \sum_{|j\rangle\in[D]} N_{fj}(T_0)\Lambda_{fj}t_j\Lambda^{\star}_{ij} \\
&= \sum_{|j\rangle\in[D]} \Lambda_{fj}t_j\Lambda^{\star}_{ij}N^{\star}_{ij}(T_0^{\dagger})
\end{aligned} \tag{47}$$

where t_j are the diagonal matrix elements of T_0 :

$$t_j \equiv t_{jj} = \langle j \mid T_0 \mid j\rangle \tag{48}$$

and

$$N_{kj}(T_0) \equiv \frac{1}{\Lambda_{kj}\langle j \mid T_0 \mid j\rangle} \sum_{|l\rangle\in[D]} \Lambda_{kl}\langle l \mid T_0 \mid j\rangle. \tag{49}$$

In order to estimate the undimensional quantities N_{kj} we rewrite (49) in the form:

$$\frac{1}{N_{kj}} = 1 - \sum_{|l\rangle\neq|j\rangle\in[D]} \Lambda_{kl}t_{lj}[\sum_{|l\rangle\in[D]} \Lambda_{kl}t_{lj}]^{-1}. \tag{50}$$

Since Λ is a 'soft' operator its matrix elements Λ_{kf} in the diffractive sector change smoothly under changes of states. Thus if the equivalence class of diffractive states $[D]$ is very rich, i.e. it contains an infinite number of states, then the second term in (50) will approach unity. This means

$$N_{kj} \equiv N \to \infty \tag{51}$$

for any pair of states $|k\rangle$ and $|j\rangle$ and leads to an enormous simplification of Eq.(46) :

$$T_{fi} = t_i\delta_{fi} - N(\Lambda_{fi}t_i + \Lambda^{\star}_{if}t_f - \sum_{|j\rangle\in[D]} \Lambda_{fj}t_j\Lambda^{\star}_{ij}). \tag{52}$$

The presence of the infinite factor N will not cause any problem since the equation can be put in the following form:

$$T_{fi} = t_i\delta_{fi} + N[\frac{1}{2}(\Lambda_{fi} - \Lambda^{\star}_{if})(t_f - t_i) + (\Lambda_{fi} + \Lambda^{\star}_{if})(t^{(fi)}_{av} - \frac{t_f + t_i}{2})] \tag{53}$$

where

$$t^{(fi)}_{av} = \frac{\sum_{|j\rangle\in[D]} \Lambda_{fj}\Lambda^{\star}_{ij}t_j}{\sum_{|j\rangle\in[D]} \Lambda_{fj}\Lambda^{\star}_{ij}} \tag{54}$$

represents an average value of the diagonal matrix elements t_j weighted with the products of the matrix elements of Λ between the initial (or final) state and the intermediate diffractive states.

We observe that the infinite value N is always accompanied by a deviation Δt which is either the difference of diagonal matrix elements between the initial and final state or the deviation of the two former from the average value over the whole set $[D]$. In the equivalence class of diffractive states which are supposed to be 'close' to each other these deviations should be very small. Therefore we require to consider the equation (53) in the following Bjorken-type limit:

$$\begin{aligned} & N \to \infty, \quad \Delta t \to 0 \\ \textit{such that} \quad & N\Delta t \quad \textit{is finite.} \end{aligned} \tag{55}$$

This can be referred to as the diffractive limit [5].

It should be noticed that in the above equations appear the T_0-diagonal matrix elements of the diffractive states only. On the other hand, the unitarity of $S_0 = 1 + iT_0$ implies the relation:

$$2\, Im(t_j) \;= |t_j|^2 \;+ \sum_{|k\rangle \neq |j\rangle} |\langle k \mid T_0 \mid j\rangle|^2 \tag{56}$$

where to the 'inelastic shadow' term in the RHS contribute both the states which are diffractive and non-diffractive. The diffractive intermediate states appear manifestly in the average value and their importance is hidden in the infinite value of N. Instead, the non-diffractive intermediate states occur only implicitly through the unitarity properties of the matrix elements t_j which are assumed to be given.

3.3 Elastic scattering and inclusive inelastic diffraction

In the case of elastic scattering Eq.(53) becomes:

$$T_{ii} \;=\; t_i \;+\; G\,(t_{av}^{(i)} - t_i) \tag{57}$$

where

$$\begin{aligned} G \;&=\; N\, g_i, \\ g_i \;&=\; \sum_{|j\rangle \in [D]} |\Lambda_{ij}|^2 \;= 2Re(\Lambda_{ii}) \end{aligned} \tag{58}$$

are the coupling constants while

$$t_{av}^{(i)} = \sum_{|j\rangle \in [D]} |w_{ij}|^2 t_j \tag{59}$$

is another average value of t_j with the weigth

$$|w_{ij}|^2 = \frac{|\Lambda_{ij}|^2}{\sum_{|k\rangle\in[D]} |\Lambda_{ik}|^2}. \tag{60}$$

The elastic scattering amplitude (57) is to be considered in the limit where the coupling constant $G \to \infty$ and

$$t_{av}^{(i)} - t_i = \sum_{|j\rangle\neq|i\rangle} |w_{ij}|^2 (t_j - t_i) \to 0 \tag{61}$$

such that the second term in (57) remains finite. We refer to this term as the diffractive contribution to elastic scattering since it originates from the action of the operator Λ which filters as intermediate states only those equivalent to the initial state. By contrast, the first term in (57) to which, as the unitarity equation (56) shows, contribute intermediate states from all possible equivalence classes, may be referred to as the non-diffractive contribution to elastic scattering. This classification of the contributions with respect to the nature of intermediate states is an approximation. In fact, in the non-diffractive term there is also a small presence of diffractive shadow and the diffractive contribution is affected by non-diffractive transitions through the properties of the diagonal elements t_j. However, the essential point is that while the non-diffractive term in elastic scattering is mostly feed by the shadow of non-diffractive transitions, in the diffractive term it is the shadow of diffractive transitions which is dominant.

It can easily be checked that the elastic diffractive contributions in the whole equivalence class [D] effectively cancel each other:

$$\sum_{|i\rangle\in[D]} g_i(t_{av}^{(i)} - t_i) = \sum_{|i\rangle,|j\rangle\in[D]} [|\Lambda_{ij}|^2 - |\Lambda_{ji}|^2] t_j = 0. \tag{62}$$

Although generally $|\Lambda_{ij}|^2 \neq |\Lambda_{ji}|^2$ the cancellation in (62) is exact. Thus the passage from the diffractive amplitude (46) to its simplified form (53) does not destroy invariance of the trace of T in the diffractive sector:

$$\sum_{|i\rangle\in[D]} T_{ii} = \sum_{|i\rangle\in[D]} t_i. \tag{63}$$

The mechanism of the diffractive limit allows us to interpret the diffractive term in elastic scattering as infinite sum of infinitesimal contributions from all intermediate states belonging to the given equivalence class of diffraction. An analogous interpretation applies to the diffractive terms in the general diffraction amplitude (53).

Making use of completness of diffractive states in the equivalence subspace one may obtain from (53) the inclusive cross-section of inelastic diffraction:

$$\sum_{|f\rangle\neq|i\rangle} |T_{fi}|^2 = N^2[\sum_{|f\rangle} |\Lambda_{if}|^2 |t_f|^2 - 2\,(\,Re(\Lambda_{ii})^2 - Re(\Lambda_{ii}) + |\Lambda_{ii}|^2)\,|t_i|^2$$
$$- |\sum_{|f\rangle} |\Lambda_{if}|^2 t_f\,|^2 - 2\,(1-2Re(\Lambda_{ii}))\,Re(t_i \sum_{|f\rangle} |\Lambda_{if}|^2 t_f^*)]. \quad (64)$$

Applying now the identity :

$$|\,\Lambda_{ii}\,|^2 + Re(\Lambda_{ii})^2 = 2[Re(\Lambda_{ii})]^2$$

and using the definitions (58) and (60), Eq.(64) can be written in the form:

$$\sum_{|f\rangle\neq|i\rangle} |T_{fi}|^2 = \frac{G^2}{g_i} \sum_{|f\rangle\in[D]} |w_{if}|^2 |t_{av}^{(i)} - t_f|^2 + \frac{1-g_i}{g_i} G^2\,|\,t_{av}^{(i)} - t_i\,|^2. \quad (65)$$

Thus the inclusive cross-section of inelastic diffraction is built of the two contributions: one which is proportional to a dispersion of the T_0-diagonal matrix elements and another which equals (up to a constant) the diffractive contribution to elastic scattering. Another way of writing this cross-section is that similar to Eq.(25):

$$\sum_{|f\rangle\neq|i\rangle} |T_{fi}|^2 = \frac{G^2}{g_i} \sum_{|f\rangle\in[D]} |w_{if}|^2 |t_f - t_i|^2 - |\,T_{ii} - t_i\,|^2. \quad (66)$$

Making use of completness of diffractive states in the equivalence subspace one may obtain from (53) the inclusive cross-section of inelastic diffraction:

$$\sum_{|f\rangle\neq|i\rangle} |T_{fi}|^2 = N^2[\sum_{|f\rangle} |\Lambda_{if}|^2 |t_f|^2 - 2\,(\,Re(\Lambda_{ii})^2 - Re(\Lambda_{ii}) + |\Lambda_{ii}|^2)\,|t_i|^2$$
$$- |\sum_{|f\rangle} |\Lambda_{if}|^2 t_f\,|^2 - 2\,(1-2Re(\Lambda_{ii}))\,Re(t_i \sum_{|f\rangle} |\Lambda_{if}|^2 t_f^*)]. \quad (64)$$

Applying now the identity :

$$|\,\Lambda_{ii}\,|^2 + Re(\Lambda_{ii})^2 = 2[Re(\Lambda_{ii})]^2$$

and using the definitions (58) and (60), Eq.(64) can be written in the form:

$$\sum_{|f\rangle\neq|i\rangle} |T_{fi}|^2 = \frac{G^2}{g_i} \sum_{|f\rangle\in[D]} |w_{if}|^2 |t_{av}^{(i)} - t_f|^2 + \frac{1-g_i}{g_i} G^2\,|\,t_{av}^{(i)} - t_i\,|^2. \quad (65)$$

Thus the inclusive cross-section of inelastic diffraction is built of the two contributions: one which is proportional to a dispersion of the T_0-diagonal matrix elements and another which equals (up to a constant) the diffractive contribution to elastic scattering. Another way of writing this cross-section is that similar to Eq.(25):

$$\sum_{|f\rangle\neq|i\rangle} |T_{fi}|^2 = \frac{G^2}{g_i} \sum_{|f\rangle\in[D]} |w_{if}|^2 |t_f - t_i|^2 - |\,T_{ii} - t_i\,|^2. \quad (66)$$

4 Phenomenological analysis of elastic and inclusive inelastic diffraction

In this Section the general theoretical formulae will be converted into calculable expressions. Our aim is two-fold: to confront theory with experiment and to compare various theoretical approaches between each other. This will be done on the example of elastic and inclusive inelastic differential cross-sections, evaluated both in the momentum space, where the releavant variable is the momentum transfer $q \equiv \sqrt{|t|}$, and in the impact parameter b-space.

4.1 Phenomenology of diffractons

The formulae considered so far have to be supplemented with a specification of their basic ingredients: the states $|j\rangle$ and the matrix elements t_j. The inelastic diffractive states will be imagined [5, 19] as built of a hadron bulk (representing the ground state $|i\rangle$) and of some quanta corresponding to diffractive excitations. The configurations of these quasi-particles (which can be called 'diffractons') are specified by a number n of constituents and their impact parameters :$|j\rangle \equiv |n; \vec{b}_1, \ldots \vec{b}_n\rangle$. For simplicity, we assume that the diffractons are independent of each other which means that the function $|w_{ij}|^2$ which is weighing the occurence of multi-particle configurations appears as a product of one-particle densities. Thus we write:

$$\sum_{|j\rangle \in [D]} |w_{ij}|^2 \cdots = \sum_{n=1}^{\infty} P_n \int d^2b_1, \cdots d^2b_n \prod_{k=1}^{n} |\psi(b_k)|^2 \cdots \tag{67}$$

where $|\psi(b_k)|^2$ is the density distribution in the impact plane. P_n denotes the probability to find the configuration of n diffractons and will be approximated by the Poisson distribution

$$P_n = \frac{\langle n \rangle^n}{n!} exp(-\langle n \rangle) \tag{68}$$

where$\langle n \rangle$ is the mean value of n. In the calculations we assume $P_0 << 1$ and begin the summation from $n = 0$. The above Ansatz follows a similar analysis of Miettinen and Pumplin [20], based on the standard form of Good-Walker formalism ($g_i = 1$). However, their multiparticle states $|j\rangle$ referred to configurations of constituent partons rather than to configurations of quasi-particles as we do.

The diagonal matrix elements of T_0 will be specified (in b-space) as follows:

$$t_i(b) = i\Gamma_0(b) \tag{69}$$

and

$$t_j(\vec{b}) = i(1 - (1 - \Gamma_0) \prod_{k=1}^{n} [1 - \gamma(\vec{b} - \vec{b}_k)]) \tag{70}$$

where Γ_0 represents the profile of the hadronic bulk and γ's correspond to diffractons. In the diffractive limit (55) only the single-particle term will be retained:

$$N(t_j - t_i) = (1 - \Gamma_0) \lim_{N\to\infty,\gamma\to 0} N \sum_{k=1}^{n} \gamma(\vec{b} - \vec{b}_k). \tag{71}$$

Our analysis, though based on the well-founded framework of Section 3, has a semi-phenomenological character. Therefore the shapes of the profiles Γ_0 , γ and of the density $|\psi(b)|^2$ are to be assumed. For simplicity, we take them as Gaussians:

$$\Gamma_0(b) = \frac{\sigma_0}{4\pi R_0^2} exp(-\frac{b^2}{2R_0^2}), \tag{72}$$

$$\gamma(b) = \frac{\sigma_\epsilon}{4\pi R_\epsilon^2} exp(-\frac{b^2}{2R_\epsilon^2}), \tag{73}$$

$$|\psi(b)|^2 = \frac{1}{2\pi(R_1^2 - R_\epsilon^2)} exp[-\frac{b^2}{2(R_1^2 - R_\epsilon^2)}]. \tag{74}$$

The parameters of these Gaussians, as well as the parameters g_i and $\langle n \rangle$, will be determined from comparison of the theory with experiment.

4.2 Analysis of elastic scattering

The application of our phenomenological recipes to the formula (57) yields the imaginary scattering amplitude (in b-space):

$$ImT_{ii}(b) = \Gamma_0 + N g_i \langle n \rangle S(b)(1 - \Gamma_0) \tag{75}$$

where the function $S(b)$, describing the average density of diffractons, is:

$$S(b) \equiv \int d^2s |\psi(s)|^2 \gamma(\vec{b} - \vec{s}) = \frac{\sigma_\epsilon}{4\pi R_1^2} exp(-\frac{b^2}{2R_1^2}). \tag{76}$$

The inspection of this expression leads to the conclusion that for description of elastic scattering 4 parameters are needed: R_0, σ_0, R_1 and

$$\sigma_1 \equiv \lim_{N\to\infty,\sigma_\epsilon\to 0} N g_i \langle n \rangle \sigma_\epsilon. \tag{77}$$

The imaginary scattering amplitude in momentum q-space is obtained by the Fourier-Bessel transform:

$$ImT_{ii}(q) = \frac{1}{2\pi} \int d^2b e^{i\vec{q}\cdot\vec{b}} ImT_{ii}(b) = \int_0^\infty dbbJ_0(qb) ImT_{ii}(b). \tag{78}$$

elastic cross-section σ_{el} and the forward logarithmic slope of elastic differential cross-section β.

The Table 1 includes the case of proton-proton elastic scattering at c.m. energy $\sqrt{s} = 4.4$ GeV [17]. Although the fit is quite good its property $\sigma_0 = \sigma_1$ and $R_0 = R_1$ says that this relatively low energy is yet outside the range of application of our approach. In fact, for higher energies we always had: $\sigma_0 >> \sigma_1$ and $R_0 > R_1$. This is reasonable since the non-diffractive effects dominate a long-range part of scattering and are characterised by large values of the effective coupling strength. The diffractive scattering, on the other hand, is governed by short distance dynamics and small values of the coupling strength.

4.3 Analysis of inclusive inelastic diffraction

The application of the prescription (67) to Eq. (66), written in terms of the Fourier-Bessel transforms of t_j's, yields the differential cross-section of inelastic diffraction in q-space as the sum of two contributions:

$$\frac{1}{2\pi}\frac{d\sigma_{dif}(t)}{d|t|} = \sum_{|f\rangle \neq |i\rangle} |T_{fi}(q)|^2 \equiv \frac{d\sigma_{coh}(q)}{d^2q} + \frac{d\sigma_{incoh}(q)}{d^2q}. \tag{82}$$

Such a structure has already been noticed in Eq. (65). The coherent cross-section σ_{coh} is proportional to the square of diffractive term in the elastic scattering amplitude:

$$\frac{d\sigma_{coh}(q)}{d^2q} = (\frac{1}{g_i} - 1)|T_{ii}(q) - t_i(q)|^2 \tag{83}$$

which, upon making use of Eq. (75), becomes:

$$\frac{d\sigma_{coh}(q)}{d^2q} = (\frac{1}{g_i} - 1)|\int dbbJ_0(qb)(1 - \Gamma_0)S(b; \sigma_\epsilon = \sigma_1)|^2. \tag{84}$$

The name of incoherent contribution is justified by its proportionality, in a leading order, to the mean value $\langle n \rangle$. It appears in the form of the double Fourier-Bessel transform:

$$\frac{d\sigma_{incoh}(q)}{d^2q} = \frac{1}{(2\pi)^2}\int d^2b_1 d^2b_2 e^{i\vec{q}\cdot(\vec{b}_1 - \vec{b}_2)}[1 - \Gamma_0(b_1)][1 - \Gamma_0(b_2)]I(\vec{b}_1, \vec{b}_2) \tag{85}$$

where the function

$$I(\vec{b}_1, \vec{b}_2) = N^2 g_i \langle n \rangle U(\vec{b}_1, \vec{b}_2) \tag{86}$$

depends on the correlation function of diffractons

$$U(\vec{b}_1, \vec{b}_2) \equiv \int d^2s|\psi(s)|^2\gamma(\vec{b}_1 - \vec{s})\gamma(\vec{b}_2 - \vec{s}) \tag{87}$$

$$= (\frac{\sigma_\epsilon}{4\pi})^2 \frac{1}{2R_1^2 - R_\epsilon^2} exp(-\frac{b^2}{2R_1^2 - R_\epsilon^2})\frac{1}{R_\epsilon^2} exp(-\frac{b'^2}{4R_\epsilon^2}) \tag{88}$$

where $\vec{b} \equiv \frac{1}{2}(\vec{b}_1 + \vec{b}_2), \vec{b}' \equiv \vec{b}_1 - \vec{b}_2$.
This choice of variables which factorizes the function $U(\vec{b}_1, \vec{b}_2,)$, facilitates also the evaluation of the integral (85). Since the major contribution to the integrand function comes from small values of b', one may approximate: $\Gamma_0(b_1) = \Gamma_0(b_2) = \Gamma_0(b)$, and $S(b_1) = S(b_2) = S(b)$. This allows to convert the integral (85) into a sum of products of single integrals.

From the inspection of the above formulae it results that for the description of inclusive inelastic diffraction only 3 parameters $g_i, \langle n \rangle$ and R_ϵ are required since the remaining parameters are to be determined from elastic scattering.

The coherent and incoherent contributions to inclusive inelastic diffraction are shown in Fig.6. At small momentum transfers the coherent contribution (dotted curve) is dominant. At the momentum transfer which corresponds to the position of the dip in elastic differential cross-section the coherent contribution becomes negligible and the incoherent term (dashed curve) dominates the inelastic diffraction at large momentum transfers. The solid curve is the sum of the two contributions. It was fitted to 30 experimental points of the data on proton-proton inelastic diffraction at the c.m. energy $\sqrt{s}$= 53 GeV [12].

In Fig.7 we present the analogous fit to the experimental data on proton-antiproton inelastic diffraction at c.m.energy $\sqrt{s}$= 546 GeV [15] (23 points). Both fits are excellent in the whole range of momentum transfer. Their parameters, together with the values of χ^2, are collected in Table 2. We give there also the values of the integrated cross-section of inelastic diffraction σ_{dif}. It is defined as twice the measured inelastic cross-section to account for diffractive dissociation of both colliding hadrons.

Although elastic and inelastic diffraction was illustrated on the examples involving protons and antiprotons, we did not discuss the connection between $p-p$ and $p-\bar{p}$ scattering [23]. A careful inspection of the experimental data in Figs 1 and 2 would reveal, in the vicinity of the dip, a significant difference between the two differential cross-sections which implies a presence of the odd charge conjugation exchange (C=-1). The corresponding amplitude contributes with opposite signs to $p-p$ and $p-\bar{p}$ scattering and differs in phase from the even-under-crossing amplitude which is dominant beyond the dip region. Since we are mainly interested in the connection between the elastic scattering and inclusive inelastic diffraction we did not touch the delicate problem of charge conjugation symmetry. However, a *joint* analysis of elastic *and* inelastic diffraction in *both* $p-p$ and $p-\bar{p}$ collisions might be very illuminating .

5 Discussion and conclusions

The numerical results presented in Section 4 will be discussed again with emphasis on the comparison of our approach based on the diffractive limit $N \to \infty$ with the classical description of Good and Walker as given in Section 2.2. We aim to convince the reader about the advantages of our method.

In order to understand better the relationship of the two approaches we rewrite their basic formulae using a unified notation. Thus for the elastic scattering amplitudes (57) and (24) one has:

$$T_{ii} = t_i + N g_i \sum_{|j\rangle \in [D]} |w_{ij}|^2 (t_j - t_i), \tag{89}$$

$$T_{ii}^{(GW)} = t_i + g_i \sum_{|j\rangle \in [D]} |w_{ij}|^2 (t_j - t_i); \tag{90}$$

while the inclusive inelastic cross-sections (66) and (25) read :

$$\sum_{|f\rangle \neq |i\rangle} |T_{fi}|^2 = N^2 g_i \sum_{|j\rangle \in [D]} |w_{ij}|^2 \, |t_j - t_i|^2 - |T_{ii} - t_i|^2, \tag{91}$$

$$\sum_{|f\rangle \neq |i\rangle} |T_{fi}^{(GW)}|^2 = g_i \sum_{|j\rangle \in [D]} |w_{ij}|^2 \, |t_j - t_i|^2 - |T_{ii}^{(GW)} - t_i|^2, \tag{92}$$

where the weigth $|w_{ij}|^2$ is normalized to unity. The two sets of formulae are almost identical except for the factor N which in the Good-Walker approach is absent. But this difference turns out to be essential. It should also be reminded that when $g_i = 1$ the Good-Walker approach re-appears in its standard form of Section 2.1.

In the Good-Walker approach we apply, instead of the diffractive limit (71), the complete multiple expansion (70) which yields the following elastic scattering imaginary amplitude:

$$Im T_{ii}^{(GW)}(b) = \Gamma_0 + g_i(1 - exp[-\langle n \rangle S(b)])(1 - \Gamma_0), \tag{93}$$

to be compared with Eq.(75). By inspection we conclude that the Good-Walker approach requires for description of elastic scattering one parameter more: $R_0, \sigma_0, R_1, \sigma_1 \equiv \langle n \rangle \sigma_\epsilon$ and additionally g_i which cannot any longer be absorbed in the definition of σ_1.

In Fig.8 we compare three curves corresponding to various theoretical descriptions. They were all fitted to the experimental data on proton-proton elastic scattering at the c.m. energy $\sqrt{s}$=52.8 GeV [11]. All the parameters are collected in Table 3. The solid curve corresponds to the approach based on the diffractive limit. The dashed curve was obtained in the Good-Walker formalism discussed above. Here it should be pointed out that the choice of the fifth parameter g_i is very ambigous. Similar fits can be obtained with very different values of g_i, rather the value of the product $g_i \sigma_1$ being important - compare the second and third row of Table 3. In particular,

if $g_i \to \infty$ then $\sigma_1 \to 0$ and the dashed curve becomes closer and closer to the solid one [5]. Thus the condition $g_i \to \infty$, being at variance with the unitarity constraint (28), may mimick the diffractive limit $N \to \infty$ which reflects the numerosity of the diffractive equivalence class. Seemingly the solid and dashed curves represent fits of equal quality. But there is an important difference since the dashed curve is characterized by multiple dips while these are absent in the solid curve, except for the single one observed experimentally. Finally, the dotted curve corresponds to the standard version of the Good-Walker approach, with $g_i = 1$ and $\Gamma_0 = 0$ as in Ref. [20]. It fits only the forward scattering part of the data and also shows multiple dips.

So far, the arguments put forward in favor of our method does not seem to be very convincing. E.g. the dotted curve in Fig.8 could be enormously improved by replacing the Gaussian form of the function $S(b)$ with a more sophisticated shape like a dipole opacity of the Chou-Yang model [4]. However, such a choice would prevent us from calculating the inclusive cross-section of inelastic diffraction. In fact, it is a *joint* analysis of elastic scattering and inelastic diffraction which decides about the success of our approach.

Passing to the analysis of the inclusive inelastic diffraction, we include the releavant formulae describing the coherent and incoherent contribution in the Good-Walker approach. Thus in place of Eq.(84) one has:

$$\frac{d\sigma_{coh}^{(GW)}(q)}{d^2q} = (\frac{1}{g_i} - 1)g_i^2 |\int dbbJ_0(qb)(1 - \Gamma_0)(1 - exp[-S(b; \sigma_\epsilon = \sigma_1)])|^2 \qquad (94)$$

while the incoherent function of Eq.(86) is replaced by:

$$I^{(GW)}(\vec{b}_1, \vec{b}_2) = g_i exp[-\langle n\rangle S(b_1) - \langle n\rangle S(b_2)](exp[\langle n\rangle U(\vec{b}_1, \vec{b}_2)] - 1). \qquad (95)$$

The measurements of the inclusive inelastic cross-section at the ISR and SPS colliders [12, 15] are perhaps not sufficiently appreciated. The angular distribution of inelastic diffraction is, in a wide range of energy, consistently characterised by two different slopes at small and large momentum transfers. The experimental results could therefore be well reproduced simply with a sum of two Gaussians described by 4 parameters: two slopes and two other parameters which fix the forward magnitude of each Gaussian. However, in our phenomenology we need only 3 parameters since the slope at small momentum transfers is already determined by the diffractive term in elastic scattering. The strength of this term in inelastic diffraction is set-up by the coupling constant g_i. So far, this constant was hidden in the definition of the cross-section σ_1 and in inelastic diffraction it appears as a new parameter at disposal.

It should be stressed that the coherent contribution (83) to the inclusive cross-section is a novelty of our approach [22]. In the standard version of the Good-Walker description (with $g_i \equiv 1$) the coherent contribution to inelastic diffraction does not appear at all. Thus in Ref.[20] the forward slope of inelastic diffraction

was explained in terms of incoherent scattering while our analysis shows that this scattering dominates in the region of large momentum transfers.

We claim that the shape of inelastic diffraction at small momentum transfers is determined by elastic scattering in the transition region between the forward peak and the diffraction minimum. This is successfully verified, as Figs 6 and 7 show, in experiment [12, 15], being a crucial evidence in favor of our formalism. On the contrary, the Good - Walker approach, even with $g_i \neq 1$, is not able to accomodate this effect. This is so because the coherent contribution to inelastic diffraction is there completely fixed (including the value of g_i) by elastic scattering. The thus determined coherent contribution,which is proportional to $(1/g_i - 1)g_i^2$, turns out, both for small and large values of g_i, to be too small and does not reproduce the inelastic cross-section at low momentum transfers as illustrated in Fig. 9.

We end with a brief recapitulation . Inelastic diffraction is a quantum phenomenon related to the existence of internal degrees of freedom of colliding hadrons. At high energies diffractive states are infinitely degenerated and are treated on the same footing as the ground state, all being the members of an equivalence class in the Hilbert space. In the classical description [10, 18] the inelastic diffraction originates from the diversity of elastic diffractive absorptions in the initial and final state Δt.But there is something more : intermediate virtual transitions. We were able to show that the multi-channel correction can be factorized. The diffraction amplitude appears as $N\Delta t$ to be taken in the 'diffractive limit': $N \to \infty, \Delta t \to 0$ such that $N\Delta t$ is finite. The resulting expressions were compared at the beginning of this Section. The two sets of formulae are 'almost' identical except for the factor $N \to \infty$. We stress again that this *'petite différence'* turns out to be essential for quantitative results.

References

[1] M. Born, Z. Physik **37** (1926) 863.

[2] W. E. Frahn, in **Diffractive Processes in Nuclear Physics** (Clarendon Press, Oxford, 1985).

[3] R. J. Glauber, in **Lectures in Theoretical Physics**, ed. by W. E. Brittin and L. G. Dunham (Interscience, New York, 1959), vol.1, p.315.

[4] T. T. Chou and C. N. Yang, Phys. Rev. **170** (1968) 1591.

[5] E. Etim, A. Małecki and L. Satta, Phys. Lett. **B 184** (1987) 99 ; also in **Proceedings of the Perugia Workshop on Multiparticle Production**, ed. by R. Hwa, G. Pancheri and Y. Srivastava (World Scientific, Singapore, 1989), p. 433.

[6] R. J. Glauber, Phys. Rev. **99** (1955) 1515;
E. L. Feinberg, J. Exp. Theor. Phys. (USRR) **29** (1955) 115;

[7] A. I. Akhiezer and A. G. Sitenko, Doklady Akad. Nauk (USRR) **107** (1956) 385, Phys. Rev. **106** (1957) 1236.

[8] K. Goulianos, Phys. Rep. **101** (1983) 169.

[9] A. Donnachie and P. V. Landshoff, Nuclear Phys. **B 244** (1984) 322; P. V. Landshoff in **Proceedings of the Perugia Workshop on Multiparticle Production**, ed. by R. Hwa, G. Pancheri and Y. Srivastava (World Scientific, Singapore, 1989), p. 409.

[10] M. L. Good and W. D. Walker, Phys. Rev.**120** (1960) 1857.

[11] K.R. Schubert, Tables of nucleon-nucleon scattering, in: **Landolt-Börnstein, Numerical data and functional relationship in science and technology**, New Series, Vol.1/9a (1979).

[12] M.G.Albrow et al., Nucl. Phys. **B 108** (1976) 1; J.C.Armitage et al., Nucl. Phys. **B 194** (1982) 365.

[13] A. Breakstone et al., Nucl.Phys. **B 248** (1984) 253, Phys. Rev. Lett. **54** (1985) 2180; N. Amos et al. Nucl.Phys. **B 262** (1985) 689.

[14] UA4 Colab., M.Bozzo et al., Phys. Lett. **B 155** (1985) 197; D. Bernard et al., Phys. Lett. **B 171** (1986) 142, Phys. Lett. **B 198** (1987) 583.

[15] D. Bernard et al., Phys. Lett. **B 186** (1987) 227.

[16] N. A. Amos et al., Phys. Lett. **B 247** (1990) 127; Phys. Rev. Lett. **68** (1992) 2433.

[17] G.G. Beznogikh et al., Nucl. Phys. **B 54** (1973) 78; C. Baglin et al., Nucl. Phys. **B 98** (1975) 365.

[18] A. Białas, W. Czyż and A. Kotański, Ann. of Phys. **73** (1972) 439.

[19] A. Małecki, Phys. Lett. **B 221** (1989) 191.

[20] H. Miettinen and J. Pumplin, Phys. Rev. **D 18** (1978) 1696.

[21] A. Martin, Lett. Nuovo Cimento **7** (1973) 811; J. Dias de Deus and P. Kroll, Acta Phys. Pol. **B9** (1978) 147.

[22] A. Małecki, Phys. Lett. **B 267** (1991) 523.

[23] M. M. Block and R. N. Cahn, Revs. Mod. Phys. **57** (1985) 563.

Figure captions

Fig. 1. The p-p elastic cross-section at c.m. energy $\sqrt{s} = 52.8$ GeV in the function of the squared momentum transfer $|t|$. The experimental data [11] are compared with the results of our approach (solid curve). The non-diffractive (dashed curve) and diffractive (dotted curve) contributions to the cross-section are shown separately. The parameters are given in the first row of Table 1.

Fig. 2. The $p-\bar{p}$ elastic cross-section at c.m. energy $\sqrt{s} = 53.0$ GeV in the function of the squared momentum transfer $|t|$. The experimental data [13] are compared with the results of our approach with (solid curve) and without (dotted curve) the real part of the scattering amplitude. The parameters are given in the second row of Table 1.

Fig. 3. The $p - \bar{p}$ elastic cross-section at c.m. energy $\sqrt{s} = 546$-630 GeV in the function of the squared momentum transfer $|t|$. The experimental data [14] are compared with the results of our approach with (solid curve) and without (dotted curve) the real part of the scattering amplitude. The parameters are given in the third row of Table 1.

Fig. 4. The $p - \bar{p}$ elastic cross-section at c.m. energy $\sqrt{s} = 546$ GeV at very low squared momentum transfers $|t|$. The experimental data [14] are compared with the results of our approach with (solid curve) and without (dotted curve) the real part of the scattering amplitude. The parameters are given in the third row of Table 1.

Fig. 5. The $p - \bar{p}$ elastic cross-section at c.m. energy $\sqrt{s} = 1800$ GeV in the function of the squared momentum transfer $|t|$. The experimental data [16] are compared with the results of our approach. The parameters are given in the fourth row of Table 1.

Fig. 6. The p-p inclusive inelastic cross-section at c.m. energy $\sqrt{s} = 53$ GeV in the function of the squared momentum transfer $|t|$. The experimental data [12] are compared with the results of our approach (solid curve). The coherent (dotted curve) and incoherent (dashed curve) contributions to the cross-section are shown separately. The parameters are given in Table 2.

Fig. 7. The $p - \bar{p}$ inclusive inelastic cross-section at c.m. energy $\sqrt{s} = 546$ GeV in the function of the squared momentum transfer $|t|$. The experimental data [15] are compared with the results of our approach (solid curve). The parameters are given in Table 2.

Fig. 8. The p-p elastic cross-section at c.m. energy $\sqrt{s} = 52.8$ GeV in the function of the squared momentum transfer $|t|$. The experimental data [11] are compared with various theoretical results.

Fig. 9. The p-p inclusive inelastic cross-section at c.m. energy $\sqrt{s} = 53$ GeV in the function of the squared momentum transfer $|t|$. The experimental data [12] are compared with the results of the Good-Walker approach (solid curve). The coherent (dotted curve) and incoherent (dashed curve) contributions to the cross-section are shown separately. The parameters are $g_i = 0.06$, $\langle n \rangle$=1.67 and R_ϵ=0.254 fm.

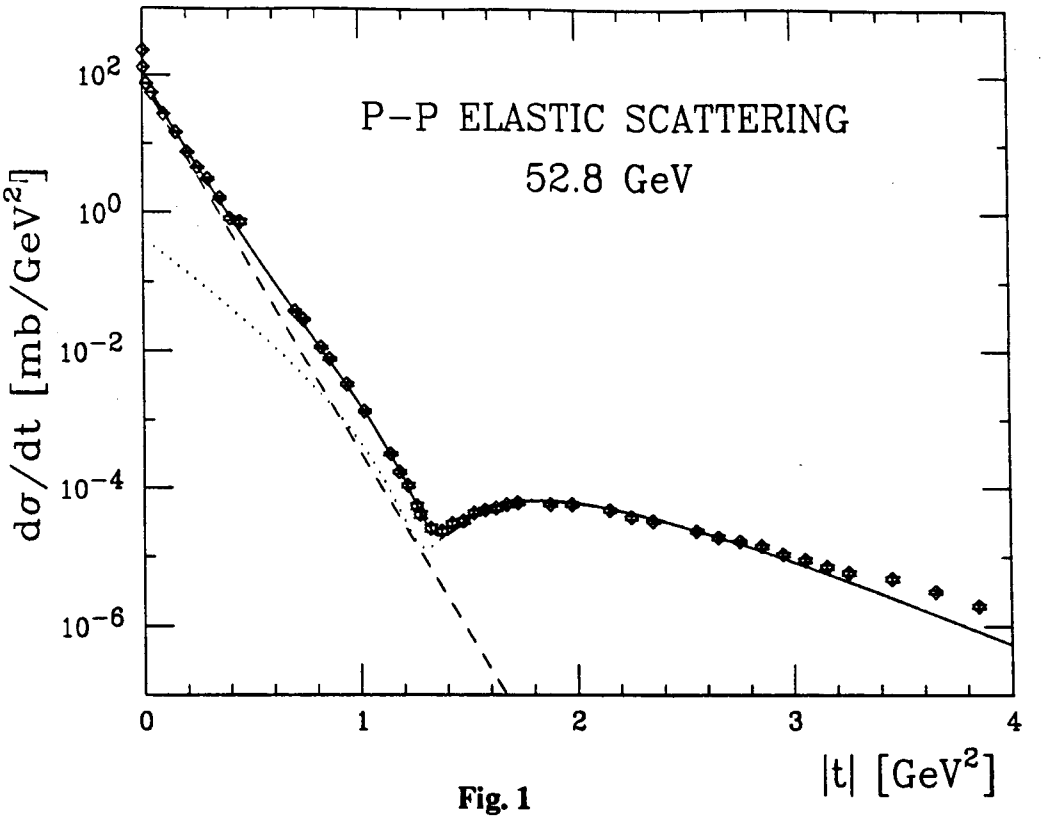
P–P ELASTIC SCATTERING
52.8 GeV
dσ/dt [mb/GeV²]
|t| [GeV²]

Fig. 1

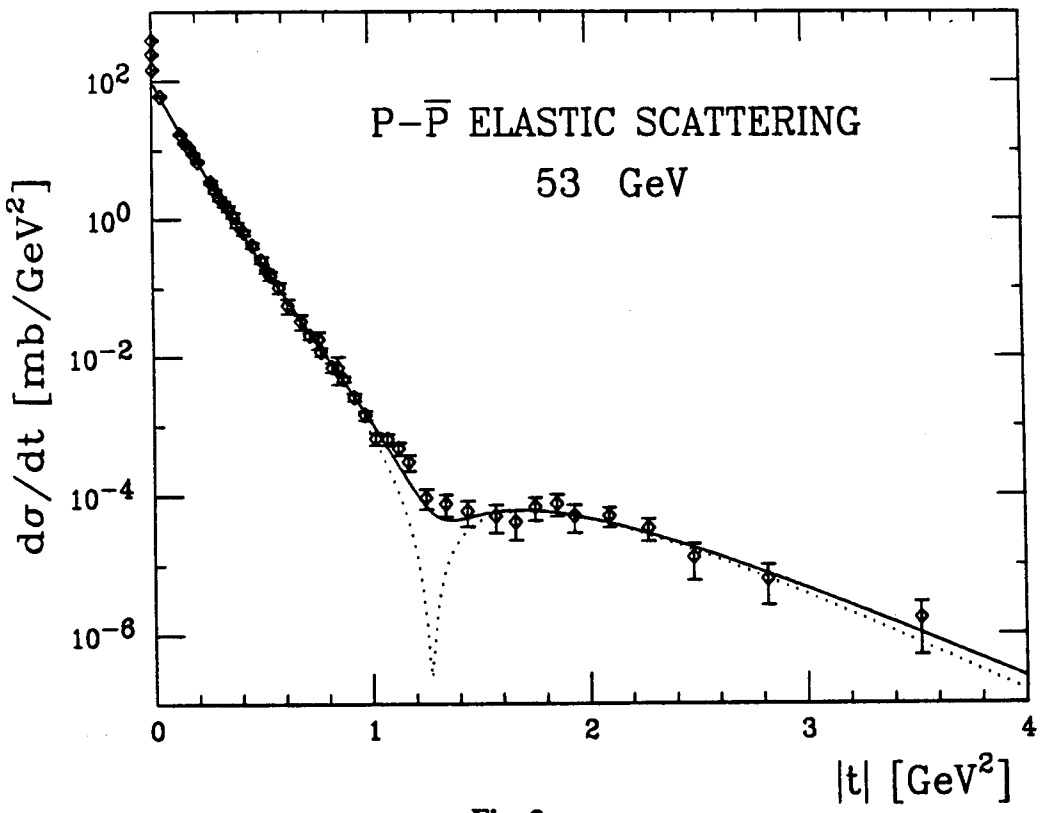
P–P̄ ELASTIC SCATTERING
53 GeV
dσ/dt [mb/GeV²]
|t| [GeV²]

Fig. 2

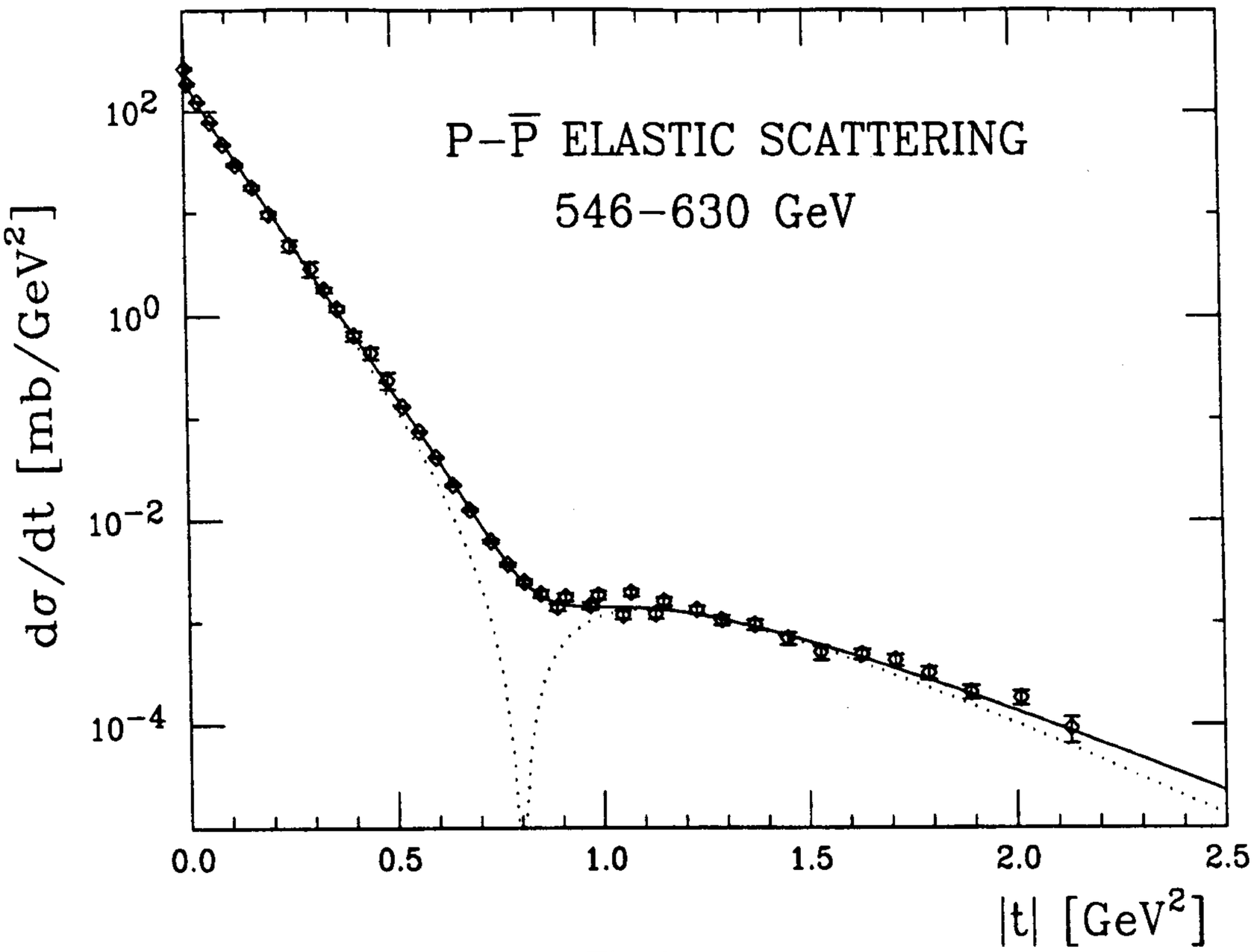
P–P̄ ELASTIC SCATTERING
546–630 GeV
dσ/dt [mb/GeV²]
10²
10⁰
10⁻²
10⁻⁴
0.0
0.5
1.0
1.5
2.0
2.5
|t| [GeV²]

Fig. 3

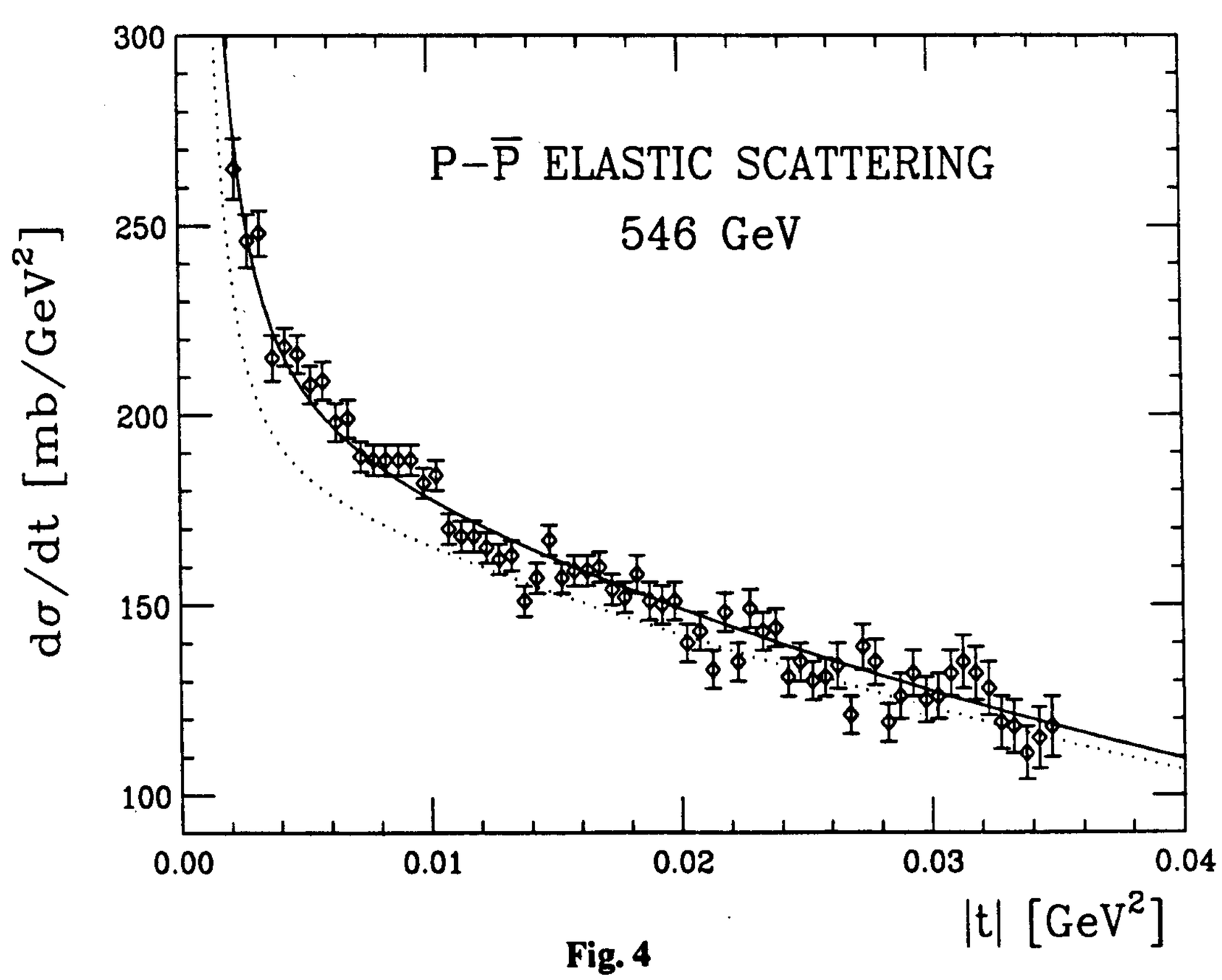
P–P̄ ELASTIC SCATTERING
546 GeV
dσ/dt [mb/GeV²]
300
250
200
150
100
0.00
0.01
0.02
0.03
0.04
|t| [GeV²]

Fig. 4

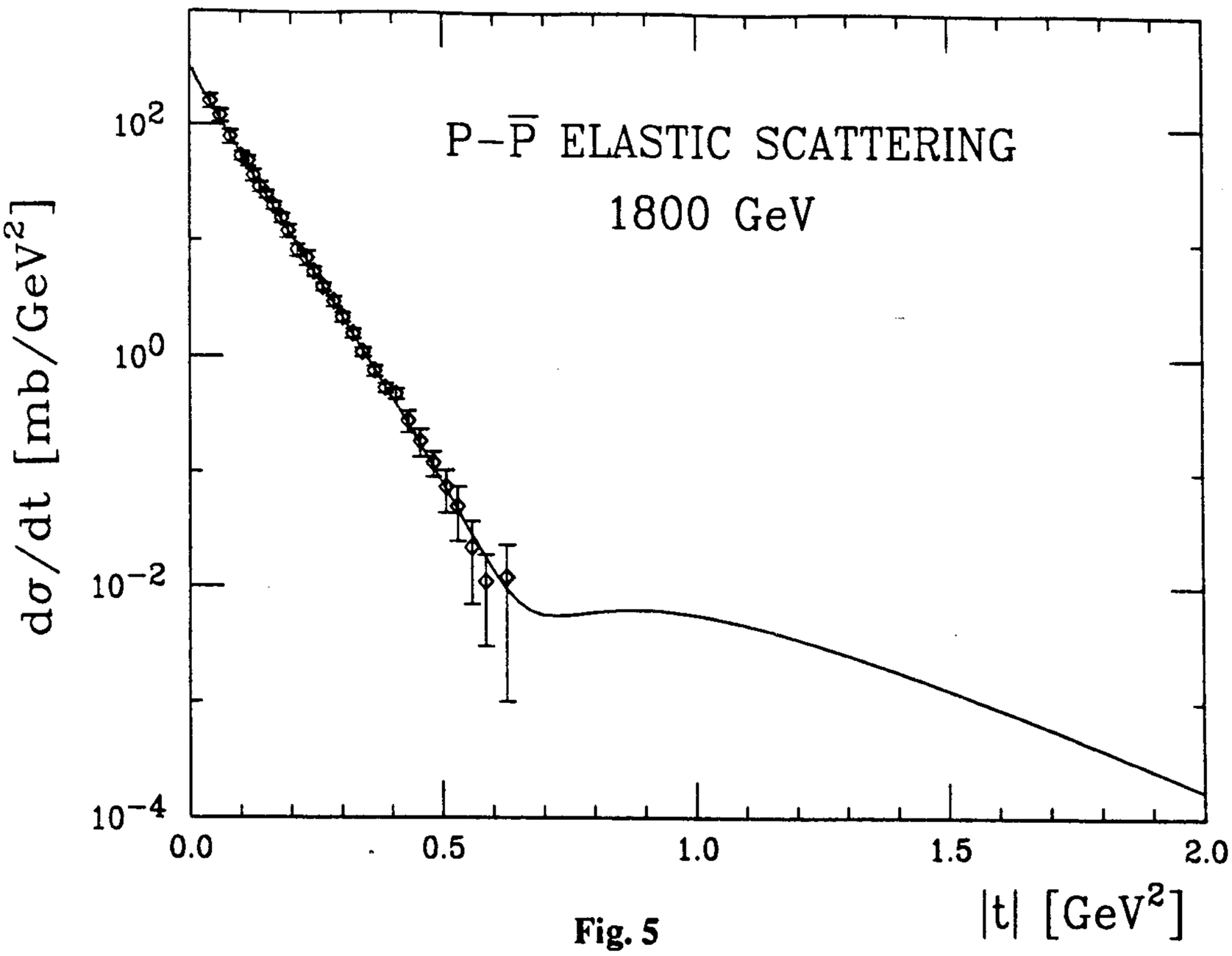
P–$\bar{P}$ ELASTIC SCATTERING
1800 GeV
$d\sigma/dt$ [mb/GeV^2]
10^2
10^0
10^{-2}
10^{-4}
0.0
0.5
1.0
1.5
2.0
|t| [GeV^2]

Fig. 5

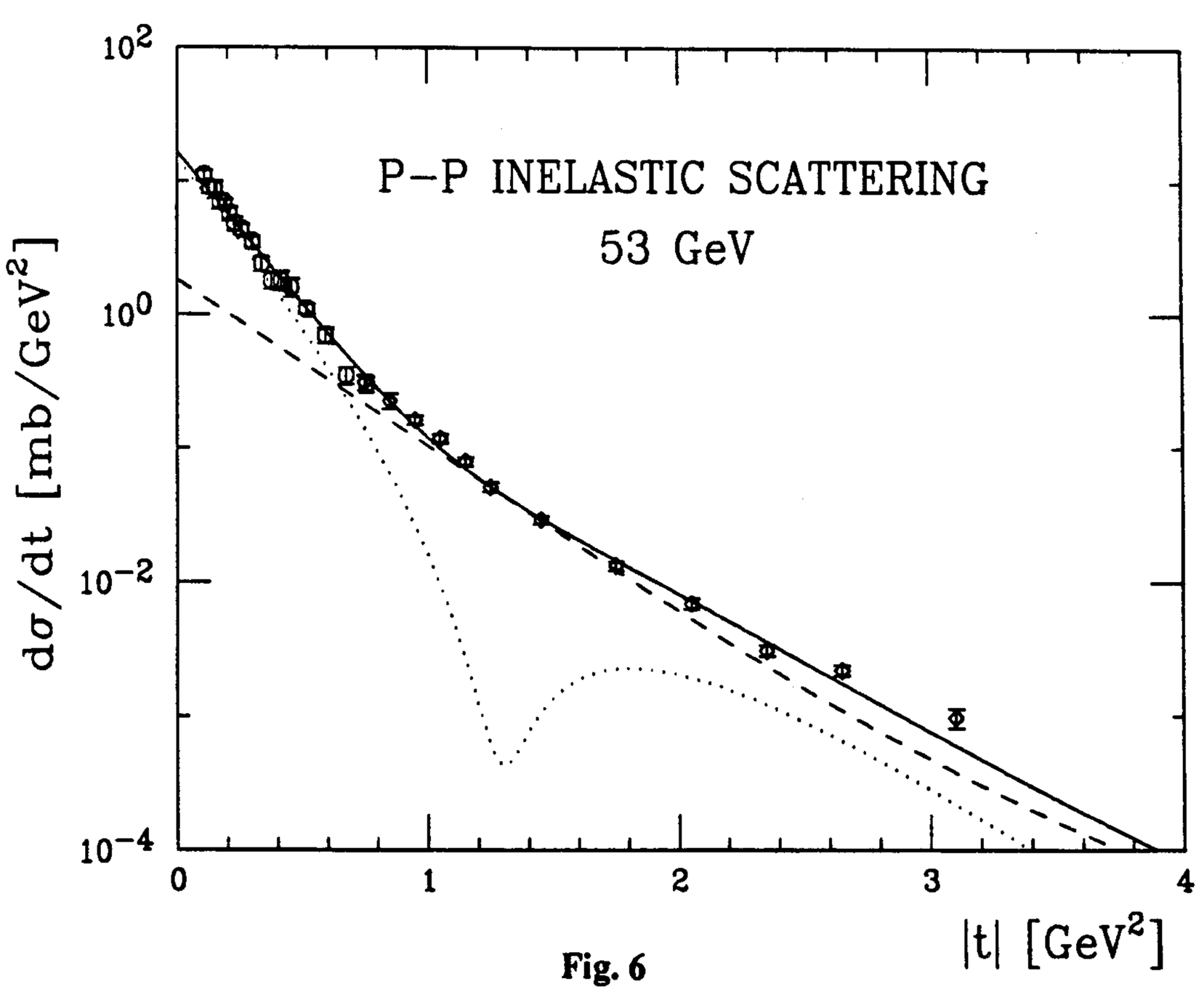
P–P INELASTIC SCATTERING
53 GeV
$d\sigma/dt$ [mb/GeV^2]
10^2
10^0
10^{-2}
10^{-4}
0
1
2
3
4
|t| [GeV^2]

Fig. 6

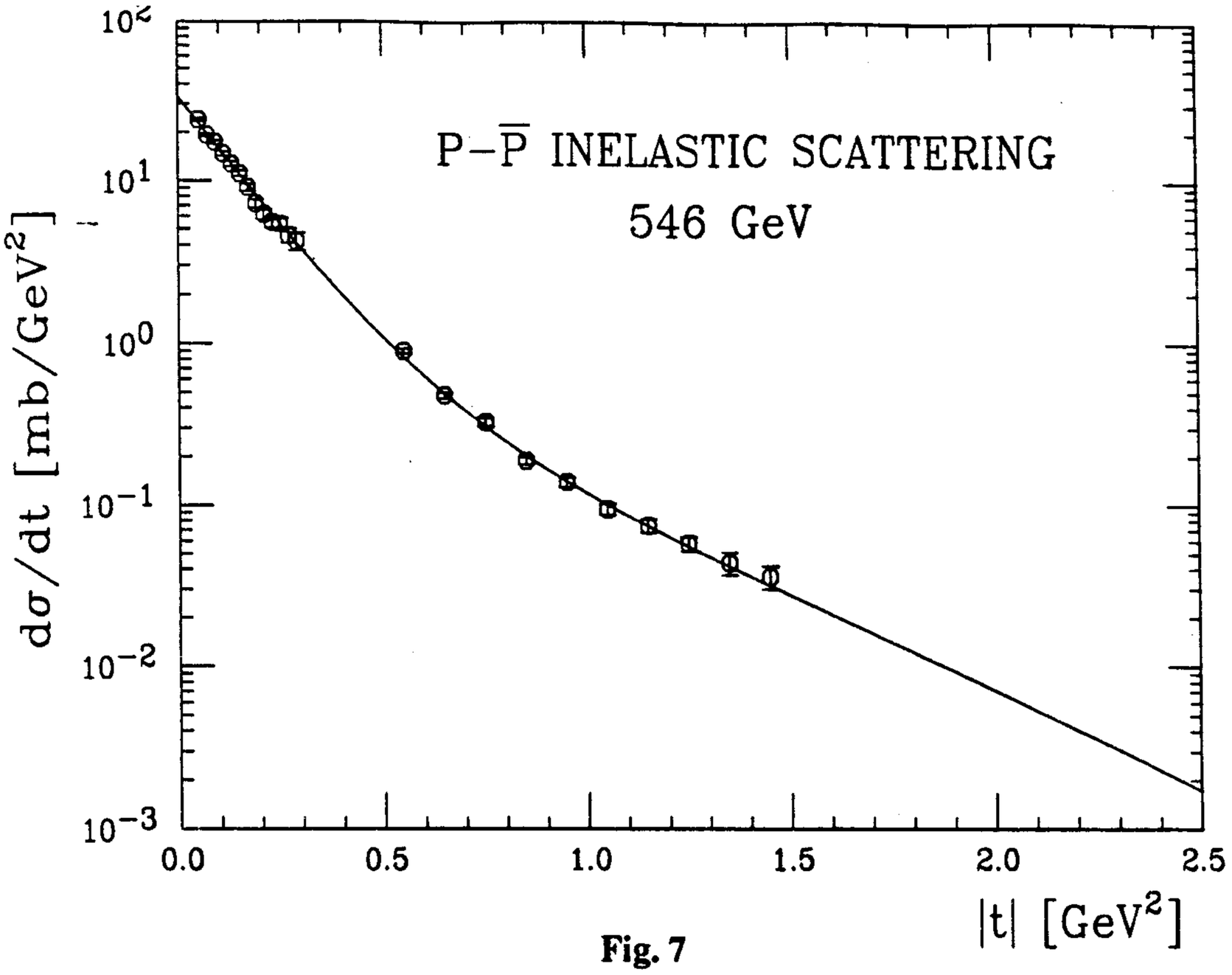
P–$\overline{P}$ INELASTIC SCATTERING
546 GeV
$d\sigma/dt$ [mb/GeV^2]
10^2
10^1
10^0
10^{-1}
10^{-2}
10^{-3}
0.0
0.5
1.0
1.5
2.0
2.5
|t| [GeV^2]

Fig. 7

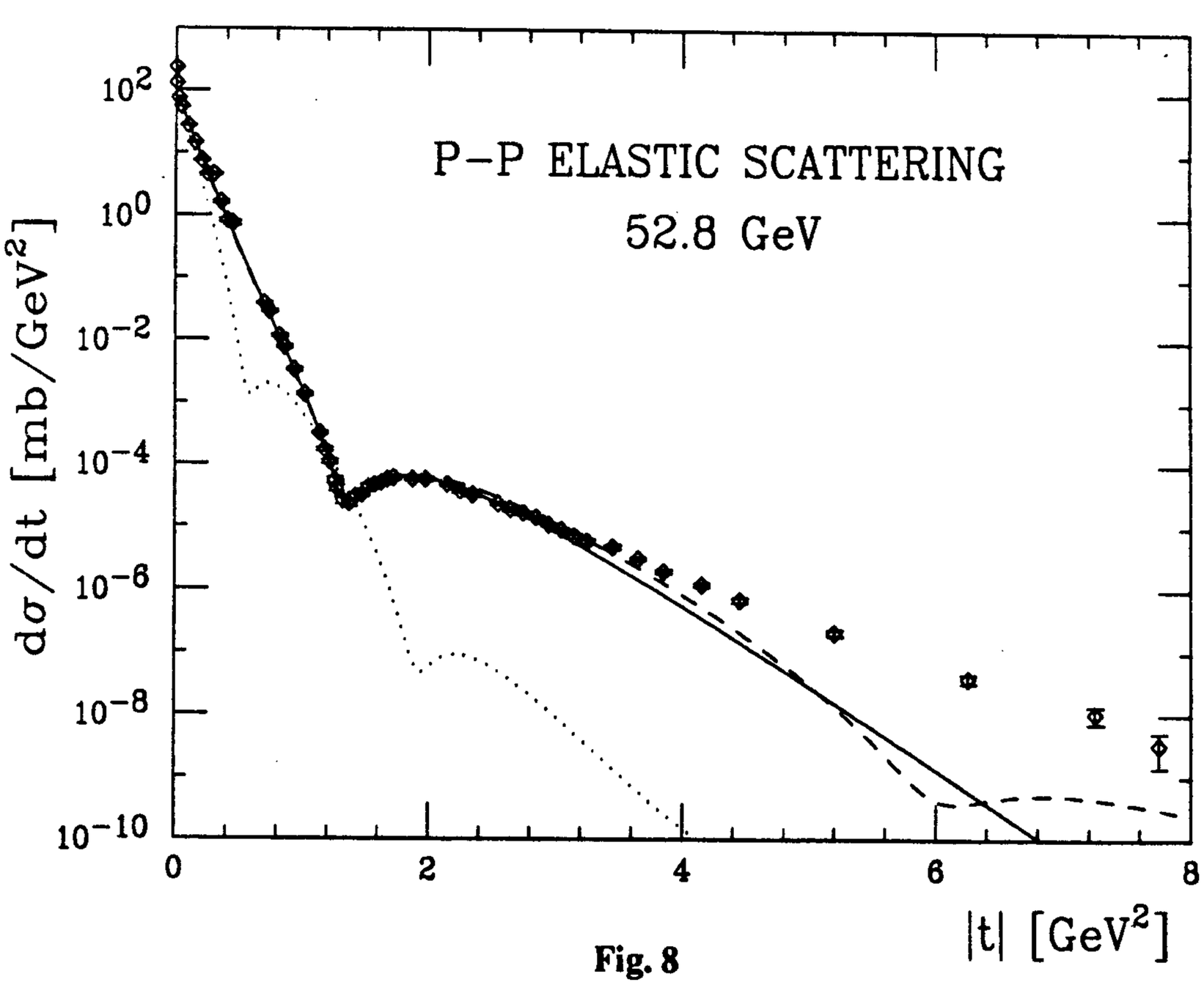
P–P ELASTIC SCATTERING
52.8 GeV
$d\sigma/dt$ [mb/GeV^2]
10^2
10^0
10^{-2}
10^{-4}
10^{-6}
10^{-8}
10^{-10}
0
2
4
6
8
|t| [GeV^2]

Fig. 8

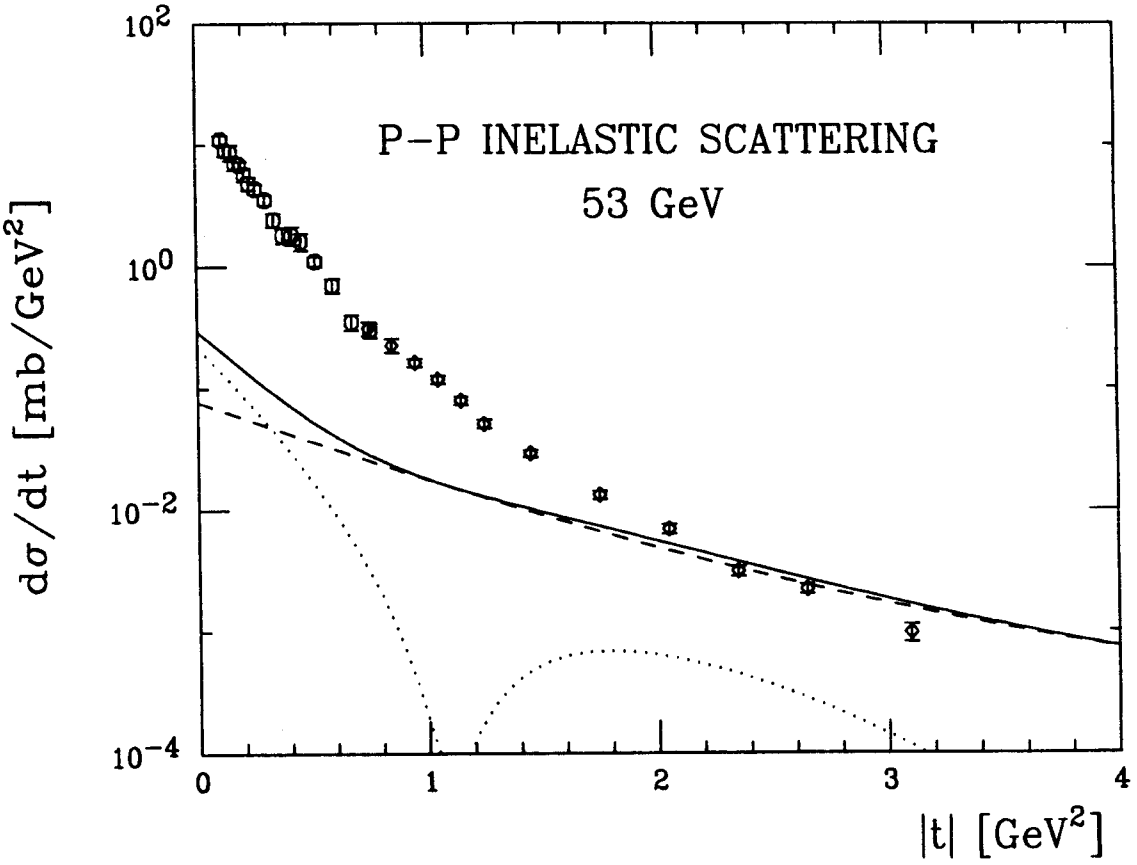
P–P INELASTIC SCATTERING
53 GeV
10^2
10^0
10^{-2}
10^{-4}
0
1
2
3
4
$d\sigma/dt$ [mb/GeV^2]
|t| [GeV^2]

Fig. 9

Table 1: The parameters of the fits presented in Figs 1, 2, 3 ,4 and 5.

Energy (GeV)	σ_0 (mb)	R_0 (fm)	σ_1 (mb)	R_1 (fm)	ρ	χ^2/df	σ_{tot} (mb)	σ_{el} (mb)	β (GeV^{-2})
p - p 52.8	39.40	0.70	5.52	0.41	0.066	80.58/39	42.29	7.74	12.04
$p-\bar{p}$ 53.0	39.37	0.72	6.15	0.44	0.13	39.54/48	42.80	7.75	12.90
$p-\bar{p}$ 546	55.78	0.76	10.71	0.51	0.194	111.8/115	60.79	13.44	14.87
$p-\bar{p}$ 1800	66.75	0.82	20.71	0.54	0.175	7.9/25	76.11	17.04	16.97
p - p 4.4	24.71	0.50	24.71	0.50	-0.36	61.21/52	39.76	11.46	8.07

Table 2: The parameters of the fits presented in Figs 7 and 8.

Energy (GeV)	g_i	$\langle n \rangle$	R_e (fm)	χ^2/df	σ_{dif} (mb)
p - p 52.8	0.0286	8.28	0.314	52.4/27	6.34
$p-\bar{p}$ 546	0.0630	1.51	0.410	29.9/20	9.32

Table 3: The parameters of the fits given in Fig.6 .

Approach	$\sigma_0(mb)$	$R_0(fm)$	$\sigma_1(mb)$	$R_1(fm)$	g_i	ρ	χ^2/df
$N \to \infty, \sigma_e \to 0$ (solid)	39.40	0.70	5.52	0.41		0.07	80.58/39
$N = 1, g_i \neq 1$ (dashed)	40.17	0.70	5.44	0.39	0.835	0.07	582.8/38
$N = 1, g_i \neq 1$ (not shown)	41.70	0.67	30.45	0.34	0.060	0.07	586.2 /38
$N = 1, g_i = 1$ (dotted)	0		51.41	0.74	1	0.09	5628.6/41